Levels in ^{154}Gd populated by the $(\alpha,2n\gamma)$ reaction and the decay of the isomers of ^{154}Tb

R. L. West,* E. G. Funk, and J. W. Mihelich
University of Notre Dame, Notre Dame, Indiana 46556
(Received 15 February 1978)

Levels in ^{154}Gd have been studied using the ^{152}Sm$(\alpha, 2n\gamma)$ reaction at an energy of 24 MeV. Singles spectra, γ-γ coincidence spectra, and angular distributions were obtained in-beam using Ge(Li) detectors. Among the new levels proposed in ^{154}Gd are as follows: a 7^+ state in the γ band; 7^-, 9^-, and 11^- states in an odd-spin octupole-vibrational band based at 1241 keV; possible 7^+ and 8^+ states in the $K^\pi = 4^+$ band based at 1646 keV; and 8^- and 9^- members of a $K = 7$ band based on the 7^- state at 2138 keV. The results are compared with various theoretical models. γ-γ directional correlation measurements were also performed on some cascades populated in the radioactive decay of the various isomers of ^{154}Tb, and the results confirm the assignment of 7^- for the 2137.8 keV state and establish a spin value of 1 for the 2119.7 and 2187.2 keV states.

NUCLEAR REACTIONS ^{152}Sm$(\alpha,2n\gamma)$, $E=24$ MeV, measured E_γ, I_γ, $\gamma\gamma$ (delay), $\gamma\gamma$ coin, $\gamma(\theta)$ ^{154}Gd deduced levels, K, J, π, δ, Q. Enriched targets. Ge(Li) detectors.
RADIOACTIVITY ^{154}Tb(22.6, 9.0, and 21.4 h) from ^{153}Eu$(\alpha, 3n)$ and ^{155}Gd$(p,2n)$. Measured $\gamma\gamma(\theta)$ ^{154}Gd deduced J, π, δ. Enriched targets. Ge(Li) detectors.

I. INTRODUCTION

With the $(\alpha, 2n\gamma)$ reaction at $\approx$25 MeV one observes sufficient side-band population to allow the study of higher-spin states in the γ band (as well as other bands). The relative population of these states is different than in the case of (HI, xn) and (α,xn) reactions at higher energies where the yrast states are populated very heavily.

From studies of the decay of ^{154}Eu (Refs. 1–4) the β- and γ-vibrational bands in ^{154}Gd have been established up to the 4^+ states, and multipole mixing parameters for transitions between low-spin states populated in the decay of ^{154}Eu have been measured by Gottel *et al.*[5] and others.[6-12] In studies of the decay of the various isomers of ^{154}Tb by Riedinger *et al.*,[13] Sousa *et al.*,[14] and Vylov *et al.*[15] the β-vibrational and γ-vibrational bands have been extended up to the 6^+ states and an I^π, $K=7^-$, 7 two-quasiparticle state with a halflife of 68 nsec has been established. This state, at 2138 keV, primarily feeds both the ground-state band and a $K^\pi=4^+$ two-quasiparticle band in which the levels had previously been established up to the 6^+ state. In-beam γ-ray investigations by Khoo *et al.*[16] and others[17-19] have extended the ground-state and β bands up to the 18^+ levels. The level structure of ^{154}Gd has also been studied via the (d,d') reaction by Bloch *et al.*[20] and the (d,t), $(^3\mathrm{He},\alpha)$, (α,t), and $(^3\mathrm{He},d)$ particle-transfer reactions by Jolly and Waddington.[21]

In the present study, γ-γ directional correlation measurements for several cascades in ^{154}Gd were carried out using radioactive sources of ^{154}Tb, and in-beam γ-ray results for ^{154}Gd were obtained from excitation function, angular distribution, and coincidence measurements using the $(\alpha, 2n\gamma)$ reaction. Several new levels are proposed, including a 7^+ state in the γ band of ^{154}Gd, possible 7^+ and 8^+ states in the $K^\pi=4^+$ band based at 1646 keV, 7^-, 9^-, and 11^- states in the $K^\pi=0^-$ band, and four high-spin states which populate the I^π, $K=7^-$, 7 state at 2138 keV. Band structure associated with the 7^-, 7 state is considered. We did not find any evidence for a so-called "superband" which was suggested by Khoo *et al.*[16] as possibly being responsible for backbending in the β-vibrational band.

II. γ-γ DIRECTIONAL CORRELATION MEASUREMENTS

A. Procedure

Two sources of ^{154}Tb were employed for the γ-γ directional correlation measurements. One source which was produced in the Notre Dame FN tandem accelerator using the $(p, 2n)$ reaction at 15 MeV was used to study transitions from the decay of the low-spin isomers, ^{154}Tb^g and ^{154}Tb^{m_1}. The second source was produced by the $(\alpha, 3n)$ reaction at 38 MeV with the cyclotron at Argonne National Laboratory and was used to study cascades involving transitions from the I^π, $K=7^-$, 7 isomeric state in ^{154}Gd which is populated in the decay of the high-spin isomer ^{154}Tb^{m_2} (22.6 h).

Two Ge(Li) detectors (20 and 40 cm^3) were placed 5 cm from the source, and a standard fast-slow coincidence circuit with $2\tau \approx 100$ nsec was utilized together with a Nuclear Data 3300 multichannel analyzer. Timing single channel analyzers and linear gates were used to decrease the signal rate at the analog-to-digital converters (ADC's) in order to minimize gain shift difficulties.

B. Results

For the first set of measurements using the source which consisted primarily of the low-spin isomers, a digital gate was set on the 123 keV ($2_g \to 0_g$) transition and data were accumulated with the detectors at angles of 90°, 135°, 180°, 225°, and 270°. Data from conjugate angles were summed. Singles spectra were obtained at the beginning of data acquisition at each angle and were used to normalize the peak intensities for the decay correction. The resulting A_2 and A_4 values are given in Table I. Corrections were made for attenuation of the coefficients resulting from the finite geometry of the system, the finite source size, and hyperfine interactions due to the 1.17 nsec half-life of the 123 keV state. The hyperfine attenuation factors g_2 and g_4 were obtained by comparing the experimental A_2 value for the well known 1291 keV $E1$ transition ($1^- \to 2^+$) and the A_4 value for the 557 keV ($0^+ \to 2^+$) $E2$ transition with the expected theoretical values.

The results for the 1997-123 and 2064-123 keV γ-γ correlations are both consistent with assignments of 1^+, but not 2^+, for the 2120 and 2187 keV levels. These were previously assigned by Sousa *et al.*[14] as 1^+ or 2^+. The experimental A_2 and A_4 values for the 1997-123 keV $1^+(D,Q)2^+(Q)0^+$ cascade limit the values of the multipole admixture for the 1977 keV transition to $0.8 \leqslant \delta \leqslant 1.35$. For the 2064-123 keV $1^+(D,Q)2^+(Q)0^+$ cascade, the values obtained for the multipole admixture of the 2064 keV transition do not quite overlap; the δ values obtained from A_2 and A_4 are $1.50^{+0.75}_{-0.45}$ and $0.69^{+0.30}_{-0.24}$, respectively. The assignment of 1^+ for the 2187 keV state is consistent with the conclusions of Jolly and Waddington[21] based on proton-transfer data. They propose a $K^\pi = 1^+$ band based on this state which they assign as the two-quasiproton configuration $\{\frac{5}{2}^+[413]_\pi - \frac{3}{2}^+[411]_\pi\}$.

The second set of angular correlation data was obtained with the $(\alpha, 3n)$ source which contained an appreciable amount of the high-spin isomer. Two transitions of primary interest were those of 993 keV ($7^-, 7 \to 8_g^+$) and 1420 keV ($7^-, 7 \to 6_g^+$). Gates were digitally set on the 346 keV ($6_g^+ \to 4_g^+$) and 427 keV ($8_g^+ \to 6_g^+$) transitions. Three sweeps were taken at 45° intervals from 90° through 270°, with additional angles of 112.5°, 157.5°, 202.5°, and 247.5° being added for the second sweep. The resulting data were normalized and analyzed in the same

TABLE I. γ-γ directional correlation results for transitions between low-spin states in ^{154}Gd populated in the decays of ^{154}Tbg ^{154}Tbm_1 and high-spin states populated in the decay of ^{154}Tbm_2.

Cascade transitions E_γ-E_γ (keV)	Assigned spin sequence	Present work A_2[a]	A_4[b]	Theoretical coefficients for assigned spin sequence A_2	A_4
^{154}Tbg, ^{154}Tbm_1					
557-123	$0^+(2)2^+(2)0^+$	0.170 (28)	1.13 (12)	0.36	1.14
1274-123	$2^-(1)2^+(2)0^+$	0.225 (25)	0.081 (81)[c]	0.250	0.0
1291-123	$1^-(1)2^+(2)0^+$	−0.248 (31)	−0.011 (99)	−0.250	0.0
1997-123	$1^+(1,2)2^+(2)0^+$	0.462 (96)	−0.46 (16)		
2064-123	$1^+(1,2)2^+(2)0^+$	0.569 (46)	−0.24 (12)		
^{154}Tbm_2					
427-346	$8^+(2)6^+(2)4^+$	0.134 (26)	0.009 (40)	0.102	0.009
1420-346	$7^-(1)6^+(2)4^+$	−0.071 (30)	−0.003 (44)	−0.071	0.0
993-427	$7^-(1)8^+(2)6^+$	−0.043 (44)	−0.099 (100)	−0.102	0.0

[a]Corrected with $g_2 = 0.87$ (5) obtained from the 1291 keV $E1$ transition in the $1^-(1)2^+(2)0^+$ cascade.

[b]Corrected with $g_4 = 0.72$ (5) obtained from the 557 keV $E2$ transition in the $0^+(2)2^+(2)0^+$ cascade.

[c]Average value of coefficient A_2 from Refs. 1, 5, 6, 7, 8 is $A_2 = 0.223(2)$.

manner as described previously and the A_2 and A_4 coefficients are presented in Table I. The 2138 keV state has been previously established by Riedinger *et al.*[13] as 7^- on the basis of internal conversion electron data for the 226 keV transition and γ-ray branching data. For a spin sequence of $7(D,Q)6(Q)4$, the 1420-346 keV correlation data are consistent with pure $E1$ ($\delta \leq 0.05$) for the 1420 keV transition. The A_2 and A_4 values for the 993-427 keV angular correlation measurement have large errors due to the composite nature of the 993 keV peak and no meaningful information can be obtained from these data.

III. IN-BEAM γ-RAY EXPERIMENTS

A. Procedure

In the in-beam ($\alpha,2n\gamma$) experiments, 24 MeV α particles from the tandem accelerator were incident on isotopically enriched ^{152}Sm targets (98.3%). These targets were produced by reducing the Sm oxide with La and then rolling the metal to a thickness of 5–10 mg/cm^2. The γ-ray data were obtained with coaxial Ge(Li) detectors having volumes of 40 and 55 cm^3 [resolution $\approx$2.2 keV full width at half maximum (FWHM) at 1332 keV]. γ-rays were assigned to ^{154}Gd on the basis of their excitation functions and coincidence sequences.

Angular distribution data for ^{154}Gd were taken at seven angles; 0, 24, 35, 45, 55, 66, and 90°. Normalization of the spectra at each angle to the same number of reactions was carried out by using a fixed monitor Ge(Li) detector. Dead-time corrections were performed using a pulser. Instrumental anisotropy and relative efficiency measurements were obtained with a radioactive source placed in the target chamber. Appreciable absorption of low energy γ rays ($\leq$200 keV) occurs at 0° because of the lead beam stop and this gives rise to a large error on the intensities.

The angular distribution data for ^{154}Gd were analyzed using a technique which compared the experimental data to the theoretical predictions based on assumed spins, m-substate population alignment parameters, and the multipole-mixing parameters δ. The above three parameters were then varied in a systematic manner until a minimum value of χ^2 was obtained, thus establishing the three parameters. The errors on these parameters can be determined from confidence levels placed on χ^2, following the method of Cline and Lesser.[22] Intensities obtained from the angular distribution data, experimental values for the A_2 and A_4 coefficients, and the parameters determined from the χ^2 analysis are listed in Table II.

For all coincidence measurements, a 40 cm^3 Ge(Li) detector was positioned at 90° and a 55 cm^3 Ge(Li) detector at $\approx$55°. The coincidence data for ^{154}Gd were obtained with three 4096 channel ADC's interfaced to the computer and recorded using computer codes in an on-line foreground/background system. One code records the data in a three parameter [$E_{\gamma 1}$, $E_{\gamma 2}$, time-to-amplitude-converter (TAC)] event mode onto magnetic tape and sorts spectra corresponding to preset gates, which it stores on disk. About 150 gates were analyzed (including off-prompt TAC gates), and typical coincidence spectra for ^{154}Gd are shown in Fig. 1. The top spectrum was obtained with the energy gate set for the full energy range (50–1850 keV) and the TAC window set for the full time range (800 nsec). It shows all peaks that are present in the coincidence spectra. The middle and lower spectra are coincidence spectra (interference subtracted) obtained with gates set on the photopeaks of interest and the appropriate section of the timing curve.

B. Results

The decay scheme for ^{154}Gd determined from this work is presented in tabular form in Table III. Alternate placements are indicated with the letter b and transitions that are composite in the singles spectra are indicated by an asterisk. Several levels having only one depopulating transition are proposed, but these are based on coincidence data. A level diagram showing the postulated band structure and other states in ^{154}Gd is shown in Fig. 2. These levels are labeled as to the reaction or activity by which they are populated.

The γ-vibrational band. Levels in the γ-vibrational band at 996.3 (2^+), 1127.9 (3^+), and 1263.9 keV (4^+) have been thoroughly studied in the decay of ^{154}Eu. (Refs. 5–12). In studies of the decay of ^{154}Tb, levels at 1432.5 and 1606.8 keV have been proposed as the 5^+ and 6^+ members of this band and the present work supports these assignments. The two transitions from the 1432.5 keV level to the 4_g^+ and 6_g^+ states have angular distributions that are consistent with a spin assignment of 5. For the 1606.8 keV state, angular distribution data could be obtained for only one transition (which feeds the 6_g^+ state) and these data were consistent with the assignment of 6^+. A newly proposed 7^+ state located at 1810.3 keV is placed on the basis of interband transitions of 665.9 keV to the 8_g^+ state and 1092.5 keV to the 6_g^+ state observed in coincidence spectra, and an intraband transition of 378 keV which feeds the 5^+, 2 state and is coincident with the $5^+,2 \rightarrow 4_g^+$ transition. Angular distribution data obtained for these three transitions are consistent with the spin assignment of 7^+ as can be seen in Fig. 3.

The energy spacings of successive spin members

TABLE II. Transition data, angular distribution coefficients, and mixing ratios for ^{154}Gd.

E_γ (keV)	Placement Init. level (keV)	Final level (keV)	I_γ [a]	A_2	A_4	Assumed spin sequence	δ [b]	σ [c]
123.1	$123(2_g^+)$	$0(0_g^+)$	97.48(74)	0.100(17)	−0.046(24)	$2\rightarrow0$	0.00(97)	$2.2^{+4}_{-2.2}$
141.0	$1912(6^+4)$	$1770(5^+4)$	2.45(3)	0.13(3)	0.068(39)	$6\rightarrow5$	$6.1^{+5.3}_{-2.2}$	3.1(30)
							$7.1^{+6.3}_{-2.6}$	2.8(30)
161.9	$2074(7^+4)$	$1912(6^+4)$	2.12	0.009(22)	0.004(32)			
166.0	2475	2309	0.79(2)	−0.93(5)	0.16(6)	$5\rightarrow6$	$1.88^{+0.59}_{-0.62}$	$0.87^{+3.00}_{-0.87}$
						$7\rightarrow6$	$-0.43^{+0.13}_{-0.23}$	$1.3^{+3.0}_{-1.3}$
						$7\rightarrow8$	$1.77^{+0.59}_{-0.62}$	$1.3^{+3.0}_{-1.3}$
						$9\rightarrow8$	$-0.44^{+0.13}_{-0.26}$	$1.7^{+3.0}_{-1.7}$
172.0	2310	$2138(7^-7)$	2.31(4)	−0.97(4)	0.006(54)	$6\rightarrow7$	$0.543^{+0.100}_{-0.007}$	$0.30^{+3.00}_{-0.30}$
						$8\rightarrow7$	$-0.394^{+0.059}_{-0.072}$	$0.280^{+3.00}_{-0.28}$
180.8	$2255(8^+4)$	$2074(7^+4)$	1.42(2)	−0.25(3)	0.001(43)			
226.0	$2138(7^-7)$	$1912(6^+4)$	2.41(2)	−0.15(2)	0.017(27)	$7\rightarrow6$	$0.031^{+0.048}_{-0.044}$	2.8(30)
							$0.017^{+0.049}_{-0.048}$	3.1(30)
232.1	$1048(4^+0')$	$816(2^+0')$	1.30(3)	0.22(5)	−0.16(6)	$4\rightarrow2$	$-0.13^{+0.13}_{-0.14}$	$1.5^{+5.0}_{-0.4}$
248.0	$371(4_g^+)$	$123(2_g^+)$	139.36(81)	0.26(1)	−0.057(18)	$4\rightarrow2$	$-0.009^{+0.022}_{-0.026}$	$1.90^{+0.15}_{-0.10}$
265.8[d]	$1911.7(6^+4)$	$1645.9(4^+4)$	~0.8					
266.0[d]	2403.8	$2137.8(7^-7)$	~1.3					
302.8[d]	2440.6	$2137.8(7^-7)$	~1.2					
303.4[d]	2073.7	$1770.3(5^+4)$	~0.8					
304.9[d]	$1911.7(6^+4)$	$1606.8(6^+\gamma)$	~0.4					
312.8			0.60(2)	0.42(8)	−0.11(11)			
318.2	$1366(6^+0')$	$1048(4^+0')$	4.51(5)	0.33(2)	−0.091(30)	$6\rightarrow4$	$-0.004^{+0.070}_{-0.066}$	$1.9^{+0.9}_{-0.5}$
329.1			0.90(10)	−0.17(22)				
338.2	$1770(5^+4)$	$1433(5^+\gamma)$	0.77(5)	0.05(15)	0.20(17)	$5\rightarrow5$	$-0.004^{+\infty}_{-\infty}$	$3.35^{+4.0}_{-3.4}$
346.7	$718(6_g^+)$	$371(4_g^+)$	100	0.30(1)	−0.077(16)	$6\rightarrow4$	$-0.009^{+0.011}_{-0.013}$	2.16(10)
378.2	$1810(7^+\gamma)$	$1433(5^+\gamma)$	1.34(2)	0.38(4)	−0.19(4)		$-0.026^{+0.048}_{-0.044}$	$1.2^{+1.0}_{-1.2}$
390.5	$1756(8^+0')$	$1366(6^+0')$	6.08(5)	0.35(2)	−0.099(25)	$8\rightarrow6$	0.00(5)	$2.16^{+0.75}_{-0.65}$
427.0	$1144(8_g^+)$	$718(6_g^+)$	52.41(27)	0.32(1)	−0.079(15)	$8\rightarrow6$	−0.004(11)	2.54(12)
	$2622(12^+0')$	$2194(10^+0')$						
437.7	$2194(10^+0')$	$1756(8^+0')$	3.39(5)	0.39(3)	−0.093(46)	$10\rightarrow8$	$0.022^{+0.081}_{-0.076}$	$2.20^{+3.0}_{-2.2}$
441.3	$2482(11^-0)$	$2041(9^-0)$	0.56(4)	0.55(15)	−0.12(20)	$11\rightarrow9$	$0.08^{+0.31}_{-0.21}$	$0.04^{+3.0}_{-0.04}$
445.0	$816(2^+0')$	$371(4_g^+)$	1.05(4)	−0.080(82)	0.20(11)	$2\rightarrow4$	$3.66^{+\infty}_{-\infty}$	$3.8(\infty)$
469.6	2780	2309	0.88(6)	0.35(13)	−0.28(15)			
479.0	$1912(6^+4)$	$1433(5^+2)$	1.01(4)	−0.39(8)	0.067(94)	$6\rightarrow5$	$-2.3^{+2.3}_{-6.5}$	3.1(31)
							or $-0.26^{+0.31}_{-9.67}$	3.1(31)
492.6	$1637(10_g^+)$	$1144(8_g^+)$	18.61(10)	0.33(1)	−0.078(16)	$10\rightarrow8$	0.00(22)	2.85(40)
518.0	$1646(4^+4)$	$1128(3^+2)$	1.99(4)	−0.16(4)	0.18(5)	$4\rightarrow3$	$-7.1^{+3.1}_{-25}$	$1.56^{+3.50}_{-0.30}$
547.5	$2185(12_g^+)$	$1637(10_g^+)$	4.10(5)	0.38(3)	−0.15(3)			
608.0	2215	$1607(6^+2)$	0.35(6)	−0.21(42)	−0.28(53)			
612.1	$1756(8^+0')$	$1144(8_g^+)$	2.01(7)	0.040(82)	−0.20(11)	$8\rightarrow8$	$-0.69^{+0.12}_{-0.14}$	$0.080^{+2.80}_{-0.08}$
648.4	$1366(6^+0')$	$718(6^+0)$	11.25(8)	0.14(1)	−0.084(19)	$6\rightarrow6$	$1.30^{+0.21}_{-0.18}$	$2.10^{+2.5}_{-2.10}$
665.9	$1810(7^+\gamma)$	$1144(8^+0)$	1.17(3)	0.25(6)	0.30(8)	$7\rightarrow8$	$-3.17^{+0.67}_{-0.99}$	$0.07^{+1.40}_{-0.07}$
676.6	$1048(4^+0')$	$371(4_g^+)$	8.01(7)	0.009(18)	−0.037(24)	$4\rightarrow4$	$2.9^{+2.10}_{-0.90}$	$2.4^{+5.0}_{-2.4}$
692.5	$816(2^+0')$	$123(2_g^+)$	4.74(7)	0.11(28)	0.061(36)	$2\rightarrow2$	$-0.02(\infty)$	$4.4^{+10.0}_{-4.4}$
715.7	$1433(5^+\gamma)$	$718(6_g^+)$	2.35(6)	−0.009(49)	−0.020(60)	$5\rightarrow6$	$-0.10^{+0.17}_{-0.20}$	$2.2^{+6.0}_{-2.2}$
							or $-6.9^{+4.2}_{-\infty}$	$2.2^{+6.0}_{-1.0}$
756.2	$1128(3^+)$	$371(4_g^+)$	2.56(6)	−0.13(5)	−0.001(58)	$3\rightarrow4$	$0.16^{+0.22}_{-0.19}$	$2.0^{+4.0}_{-2.0}$
							or $21^{+\infty}_{-17}$	$2.0^{+4.0}_{-2.0}$

TABLE II. (*Continued*)

E_γ (keV)	Placement Init. level (keV)	Final level (keV)	I_γ [a]	A_2	A_4	Assumed spin sequence	δ [b]	σ [c]
843.6	3153	2310(8^-7)	1.32(5)	−0.08(7)	0.30(8)			
845.5	2482(11^-0)	1637(10_g^+)	2.16(5)	−0.21(4)	0.052(43)	$11 \to 10$	0.05(5)	$0.17^{+2.50}_{-0.17}$
							or −0.017(35)	$0.68^{+2.50}_{-0.68}$
873.3	996($2^+\gamma$)	123(2_g^+)	5.84(10)	−0.17(3)	−0.085(39)			
	2787	1912(6^+4)						
889.6	1607($6^+\gamma$)	718(6_g^+)	3.73(4)	−0.29(2)	−0.14(3)	$6 \to 6$	$-3.1^{+1.3}_{-\infty}$	$2.22^{+0.4}_{-0.7}$
							or >7	2.10(30)
893.3	1264($4^+\gamma$)	371(4_g^+)	5.88(5)	−0.26(2)	−0.004(20)	$4 \to 4$	$-1.96^{+0.78}_{-11.5}$	$1.96^{+0.45}_{-0.65}$
896.2	2041(9^-0)	1144(8_g^+)	4.64(5)	−0.28(2)	0.053(29)	$9 \to 8$	0.017(35)	$0.77^{+3.0}_{-0.77}$
							or 0.00(4)	2.0(20)
						$7 \to 8$	0.04(5)	$1.02^{+2.0}_{-1.02}$
924.1	1048($4^+0'$)	123(2_g^+)	2.54(6)	0.16(4)	−0.18(5)	$4 \to 2$	$-0.2^{+1.3}_{-2.7}$	$1.60^{+1.00}_{-0.60}$
956.4	1674(7^-0)	718(6_g^+)	2.95(9)	−0.43(6)	0.049(48)	$5 \to 6$	$5.1^{+4.4}_{-1.9}$	$1.75^{+6.0}_{-0.88}$
							or 0.16(9)	$1.3^{+1.0}_{-1.3}$
						$7 \to 6$	−0.070(71)	$1.6^{+1.0}_{-1.6}$
957.3			2.14(7)	−0.10(6)	0.003(58)			
993.0	2138(7^-7)	1144(8_g^+)	1.87(7)	0.049(78)	0.003(87)	$7 \to 6$	$-0.16^{+0.16}_{-0.23}$	$2.5^{+4.0}_{-2.5}$
994.9	1366($6^+0'$)	371(4_g^+)	3.49(8)	0.21(5)	0.041(56)	$6 \to 4$	$0.04^{+0.21}_{-0.23}$	$2.76^{-4.0}_{-1.2}$
996.3	996($2^+\gamma$)	0(0_g^+)	2.33(6)	0.19(5)	0.046(60)	$2 \to 0$	0.00(89)	$1.54^{+0.66}_{-0.54}$
1005.0	1128($3^+\gamma$)	123(2_g^+)	8.76(7)	−0.11(2)	0.092(20)	$3 \to 2$	$-6.0^{+1.1}_{-1.6}$	$1.53^{+0.40}_{-0.25}$
1033.2			4.69(7)	−0.31(3)	0.052(37)			
1039.2	1756($8^+0'$)	718(6_g^+)	4.52(8)	0.35(4)	−0.002(47)	$8 \to 6$	$0.06^{+0.15}_{-0.13}$	$2.6^{+4.0}_{-2.6}$
1062.2	1433($5^+\gamma$)	371(4_g^+)	6.76(11)	−0.34(3)	0.20(4)	$5 \to 4$	$-4.3^{+1.2}_{-2.6}$	$1.73^{+0.65}_{-0.48}$
1092.5	1810($7^+\gamma$)	718(6_g^+)	5.17(9)	−0.61(4)	0.26(3)	$7 \to 6$	$-2.71^{+0.46}_{-0.61}$	$1.89^{+0.80}_{-0.60}$
1419.7	2138(7^-7)	718(6_g^+)	1.21(6)	0.11(9)	−0.02(11)			
1421.3	2787	1366($6^+0'$)	2.93(6)	0.066(41)	−0.100(52)			

[a]The errors quoted in parentheses represent statistical counting errors only and do not include other contributions such as the uncertainty (≥5%) in the relative efficiencies.

[b]For $\Delta I = 1$ sequences, the δ value refers to a dipole-quadrupole mixture while for $\Delta I = 2$ sequences it refers to a possible quadrupole-octupole mixture. The sign convention employed is that obtained using emission matrix elements.

[c]σ denotes the half-width of the magnetic-substate distribution for the level from which this transition proceeds.

[d]For these transitions which are not directly resolved, the energies are deduced from the placement made on the basis of coincidence data.

of the γ band of ^{154}Gd exhibit an odd-even staggering effect if $\Delta E/2I$ is plotted vs $2I^2$ as in Fig. 4. This staggering indicates a deviation from the dependence described by the expression

$$E = E_0 + AI(I+1) + BI^2(I+1)^2. \tag{1}$$

If one carries out an energy fit using the 2^+ through 6^+ states and the equation

$$E = E_0 + A[I(I+1) - K^2] + B[I(I+1) - K^2]^2 + C[I(I+1) - K^2]^3 + (-1)^I (I-1)I(I+1)(I+2) \times [A_{2K} + B_{2K}(I(I+1) - K^2)] \tag{2}$$

including only one alternating term described by the coefficient A_4, the prediction for the 7^+ state is 1797 keV, which is reasonably near the proposed state at 1810.3 keV.

A weighted least-squares fit using Eq. (2) and the energies of the 2^+ through 7^+ states yields the band parameters given in Table IV. Uncertainties in the energies of the levels in the γ band have been assigned as follows; 0.2 keV for the 2^+ through 5^+ states; and 0.5 keV for the 6^+ and 7^+ states. The resulting B_4 and C coefficients are small compared to the A_4 and B coefficients, respectively. The A

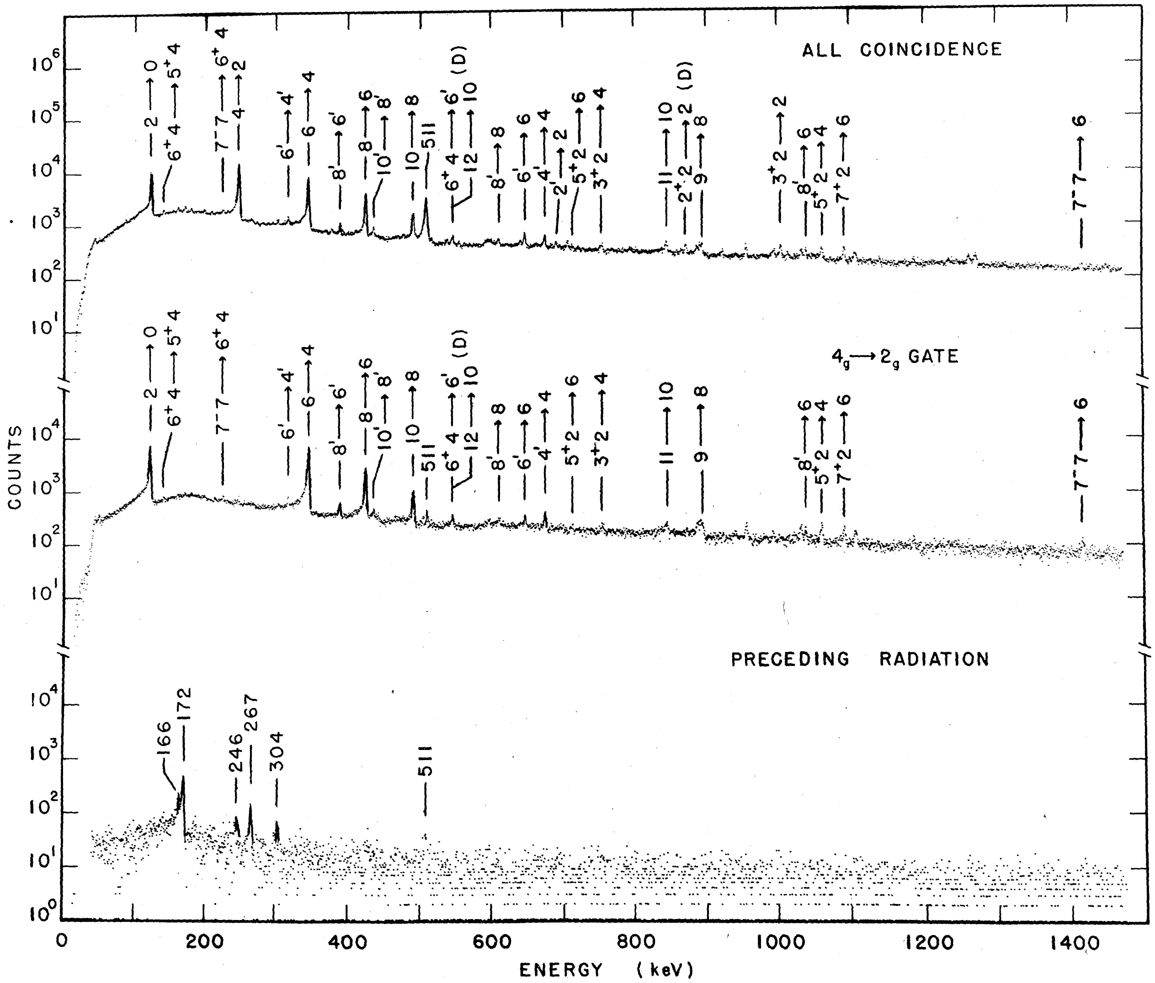

FIG. 1. γ-γ coincidence spectra obtained with the ^{152}Sm $(\alpha, 2n)$ ^{154}Gd reaction at 24 MeV. The top spectrum shows all peaks present in the coincidence spectra and was obtained with the energy gate set for 50–1850 keV and the TAC window set for the full time range of 800 nsec. The middle spectrum shows prompt coincidences with the 248 keV $(4_g^+ \rightarrow 2_g^+)$ transition and the bottom spectrum shows radiation preceding the 68 nsec state at 2138 keV; these have been corrected for interferences. Peaks marked with (D) are doublets.

coefficient for this band is 24.3 (1) keV which differs by only 12% from the value of 21.4 (1) keV for the ground-state band. If one uses the coefficients determined from the 2^+ through 7^+ states in the γ band, the 8^+ state is predicted to be at 2392 keV but there is no experimental evidence for such a state.

$K^\pi = 4^+$ band at 1645.9 keV. The 4^+, 5^+, and 6^+ levels in this $K=4$ band have been previously established from decay studies of ^{154}Tb (Refs. 13 and 14) and the bandhead has been assigned as a $\{\frac{3}{2}^+[411] + \frac{5}{2}^+[413]\}$ state. Our coincidence data indicate two possible candidates, at 2074 and 2117 keV, for the 7^+ member of this band. Since a 2117 keV state is populated much more strongly than the $6^+, 4$ level in the proton-transfer experiments,[21] while the 2074 keV state is not observed, the 2074 keV state is the more probable candidate for the $7^+, 4$ state of this band.

The 2074 keV state is based only on the observation of one weak coincident transition to the $6^+, 4$ state, and the 2255 keV $(8^+, 4)$ state is tentatively placed on the basis of two weak depopulating coincident transitions to the 7^+, 4 and 8_g^+ states in addition to three coincident transitions populating the state. No angular distribution data could be obtained.

If one uses the energies of the 4^+, 5^+, and 6^+ states and Eq. (1), the 7^+ and 8^+ states are predicted to be at 2066 and 2288 keV. If the energies of the possible 7^+ and 8^+ states are included as well, the band parameters shown in Table IV are

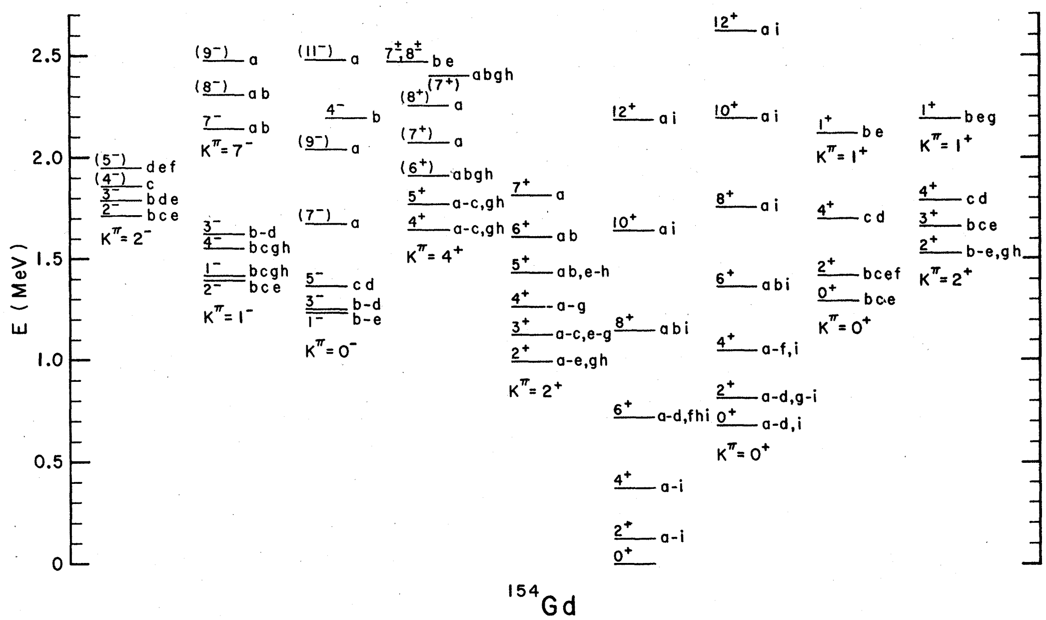

FIG. 2. Band structure in ^{154}Gd. Levels are labeled as to method of observation: (a) present work; (b) decay of ^{154}Tb (Ref. 14); (c) decay of ^{154}Eu (Ref. 4); (d) (d,d') reaction (Ref. 20); (e) (d,t) reaction (Ref. 21); (f) (^{3}He,α) reaction (Ref. 21); (g) (α,t) reaction (Ref. 21); (h) (^{3}He,d) reaction (Ref. 21); and (i) (α,xn) reaction (Ref. 16).

TABLE III. Proposed decay scheme for ^{154}Gd. Underlined transitions are placed with coincidence experiments. Asterisks indicate that the transition is part of a doublet peak in the spectrum, while *t indicates it is part of a triplet peak. For those transitions which are not directly resolved, the energies are deduced from the placement made on the basis of coincidence data. Transitions marked with a b have alternative placements in the decay scheme. The quantities in brackets [ ] are relative intensities of depopulating photons obtained from angular distribution measurements arbitrarily normalized to unity for the most intense transition from the initial state.

Level	I^π,K	Depopulating transitions (final level) (keV)	Populating transitions (initial level) (keV)
0	$0^+,0$		123.1(123.1),815.5(815.5),996.3(996.3)
123.1	$2^+,0$	123.1 (g.s.)	248.0(371.1), 692.5(815.5), 873.3* (996.3), 924.1(1047.7),1005.0(1127.9),1140.8 (1263.9)
371.1	$4^+,0$	248.0(123.1)	346.7(717.8),445.0(815.5),676.6(1047.7) 756.2^b(1127.9),893.3(1263.9), 994.9 (1365.9),1062.2(1432.5),1235.3(1606.8), 1541.2(1911.7)
717.8	$6^+,0$	346.7(371.1)	427.0(1144.4),648.4*(1365.9),715.7 (1432.5),889.6(1606.8),956.4(1674.4), 1039.2(1756.2),1092.5(1810.3),1194.0 (1911.7),1419.7(2137.8)
815.5	$2^+,0'$	445.0[1.0](371.1),692.5 [0.26](123.1),815.5(g.s.)	232.1(1047.7)
996.3	$2^+,2$	873.3*(123.1),996.3(g.s.)	649.5*(1645.9)
1047.7	$4^+,0'$	232.1[0.16](815.5),676.6 [1.0](371.1),924.1[0.32](123.1)	318.2(1365.9)

TABLE III. (*Continued*)

Level	I^π, K	Depopulating transitions (final level) (keV)	Populating transitions (initial level) (keV)
1127.9	$3^+, 2$	756.2[b][0.27](371.1),1005.0 [1.0](123.1)	518.0(1645.9),642.3(1770.3)
1144.4	$8^+, 0$	427.0(717.8)	492.6(1637.0),612.1(1756.2),665.9 (1810.3),896.2(2041.0),993.0(2137.8), 1110.0*(2254.5)
1263.9	$4^+, 2$	893.3(371.1),1140.8(123.1)	506.4(1770.3)
1365.9	$6^+, 0'$	318.2[0.40](1047.7),648.4*[1.0] (717.8),994.9[0.31](371.1)	390.6(1756.2),546.7*(1911.7),886.5[b] (2254.5),943.0(2309.5),1109.0*(2474.8), 1421.3(2786.6)
1432.5	$5^+, 2$	715.7[0.35](717.8),1062.2[1.0] (371.1)	338.2(1770.3),378.2(1810.3),479.0 (1911.7)
1606.8	$6^+, 2$	889.6(717.8),1235.3(371.1)	304.9*′(1911.7),608.0(2215.4),1088.1 (2695.9)
1637.0	$10^+, 0$	492.6(1144.4)	547.5*(2184.5), 556.8(2193.8), 635.0 (2272.8), 846.5(2482.3)
1645.9	$4^+, 4$	518.0(1127.9), 649.5*(996.3)	124.4*(1770.3), 265.8*(1911.7)
1674.4	$(7^-, 0)$	956.4(717.8)	
1756.2	$8^+, 0'$	390.6[1.0](1365.9), 612.1[0.33] (1144.4), 1039.2[0.74] (717.8)	437.6(2193.8), 459.5(2215.4)
1770.3	$5^+, 4$	124.4*(1645.9), 338.2(1432.5), 506.4(1263.9), 642.3(1127.9)	141.0(1911.7), 303.4*′(2073.7)
1810.3	$7^+, 2$	378.2[0.26](1432.5), 665.9[0.23] (1144.4), 1092.5[1.0](717.8)	886.5[b](2695.9)
1911.7	$6^+, 4$	141.0[1.0](1770.3), 265.8*[0.34] (1645.9), 304.9*′[0.15](1606.8), 479.0 [0.41](1432.5), 546.7*(1365.9), 1194.0 (717.8), 1541.2(371.1)	161.9(2073.7), 205.4(2117.1), 226.0 (2137.8), 412.8(2323.9), 756.2[b](2669.4) 873.3*(2786.6)
2041.0	$(9^-, 0)$	896.2(1144.4)	441.3(2482.3), 695.5(2735.4)
2073.7	$(7^+, 4)$	161.9[1.0](1911.7), 303.4*′[0.35] (1770.3)	172.1*(2245.8), 180.8(2254.5), 199.3 (2272.8),707.5(2779.9)
2117.1		205.4(1911.7)	
2137.8	$7^-, 7$	226.0[1.0](1911.7), 993.0[0.78] (1144.4), 1419.7[0.50](717.8)	172.0*(2309.5), 266.0*(2403.8), 302.8*′ (2440.6)
2184.5	$12^+, 0$	547.5*(1637.0)	
2193.8	$10^+, 0'$	437.6(1756.2), 556.8(1637.0)	427.8*(2621.6)
2215.4		459.5(1756.2), 608.0(1606.8)	
2245.8		172.1*(2073.7)	158.0(2403.8)
2254.5	$(8^+, 4)$	180.8(2073.7), 886.5[b](1365.9) 1110.0*(1144.4)	150.6(2403.8), 219.6(2474.8), 414.9 (2669.4), 525.4(2779.9)
2272.8		199.3(2073.7), 635.0(1637.0)	
2309.5	$(8^-, 7)$	172.0*(2137.8), 943.0(1365.9)	131.6(2440.6), 166.0(2474.8), 469.9 (2779.9), 843.6(3153.2)
2323.9		412.8(1911.7)	
2403.8	$(7^+, 7)$	150.6(2254.5), 158.0(2245.8), 266.0*(2137.8)	
2440.6		131.6(2309.5), 302.8* (2137.8)	712.4(3153.2)
2474.8	$(9^-, 7)$	166.0(2309.5), 219.6(2254.5), 1109.0*(1365.9)	221.0(2695.9), 246.2(2721.0), 260.6 (2735.4), 314.2(2786.6)
2482.3	$(11^-, 0)$	441.3[0.26](2041.0), 845.5 [1.0](1637.0)	

TABLE III. (*Continued*)

Level	I^π,K	Depopulating transitions (final level) (keV)	Populating transitions (initial level) (keV)
2621.6	12^+, 0′	427.8(2193.8)	
2669.4		414.9(2254.5), 756.2[b](1911.7)	
2695.9		221.0(2474.8), 886.5[b](1810.3) 1088.1(1606.8)	
2721.0		246.2(2474.8)	
2735.4		260.6(2474.8), 695.5(2041.0)	
2779.9		469.9(2309.5), 525.4(2254.5), 707.5(2073.7)	
2786.6		314.2(2474.8), 873.3*(1911.7), 1421.3(1365.9)	
3153.2		712.4(2440.6), 843.6(2309.5)	

obtained from a least-squares fit to Eq. (2). The plot of $\Delta E/2I$ vs $2I^2$ is presented in Fig. 4 and shows no odd-even staggering effect.

The inertial parameter $A = 12.9$ keV is considerably different from the value of ≈21 keV for the ground-state band, implying a much larger moment of inertia for the two-quasiparticle state. The expected difference can be estimated by using the A values obtained from bands in ^{153}Eu (Ref. 23) built on the $\frac{3}{2}^+[411]_p$ and $\frac{5}{2}^+[413]_p$ states, assuming that $A = \hbar^2/2\mathcal{I}$ and that $\mathcal{I}$ for an odd-A nucleus is approximately equal to the sum of $\mathcal{I}$ for the even-even core and $\delta\mathcal{I}$, the increase in $\mathcal{I}$ due to the single quasiparticle. Knowing the $\delta\mathcal{I}_{[413]_p}$ and $\delta\mathcal{I}_{[411]_p}$ values, the moment of inertia for the two-quasiparticle state can then be estimated from $\mathcal{I}\text{core} + \delta\mathcal{I}_{[413]_p} + \delta\mathcal{I}_{[411]_p}$. Using ^{152}Sm as the core, one obtains a value of $A \cong \hbar^2/2\mathcal{I}_{2qp} \cong 11$ keV, in reasonable agreement with the experimental value of ≈13 keV. This calculation ignores the interaction between the two particles which would tend to make $\mathcal{I}$ smaller and A larger, but the additional blocking effect might counteract this somewhat.

$K^\pi = 0^-$ band at 1241.3 keV. Three states at 1241.3 (1^-), 1251.7(3^-) keV, and 1364.2 keV (5^-) have been previously assigned as members of a $K^\pi = 0^-$ octupole-vibrational band on the basis of ^{154}Eu decay studies[4,9] and the inelastic deuteron scattering results of Bloch *et al.*[20] These levels were not populated in the present work, but states having possible assignments of 7^-, 9^-, and 11^- are placed at 1674.4, 2041.0, and 2482.3 keV, respectively, on the basis of coincidence measurements and angular distribution data. A partial decay scheme is shown in Fig. 5. The 7^- state is placed on the basis of a single coincident transition of 956 keV feeding the 6_g^+ state, and the angular distribution data are consistent with the spin assignment of 7 and a pure dipole transition. The 9^- and 11^- states are based on the observation of coincident transi-

TABLE IV. Band parameters for ^{154}Gd.

Band (K^π)	0^+g	$0^{+\prime}$	$2^+\gamma$	4^+	7^-
Band-head energy (keV)	0	680.7	996.3	1645.9	2137.8
Maximum $I^{\pi\,a}$	6^+	6^+	7^+	8^+	9^-
A (keV)	21.6(1)	24.9(1)	24.3(1)	12.9(2)	12.1(1)
B (eV)	−193.3(22)	−439.7(26)	−328.8(44)	−34.2(69)	−45.5(21)
C (eV)	2.0(1)	5.6(1)	3.7(1)	0.2(1)	
A_{2K} (eV)			30.1(1)	$0.1(1) \times 10^{-3}$	
B_{2K} (eV)			0.8(1)		

[a]Spin and parity of state of highest spin included in least-squares fit to Eq. (2). The alternating terms involving both A_{2K} and B_{2K} were included for the $K = 2\gamma$ band and the A_{2K} term only for the $K = 4$ band.

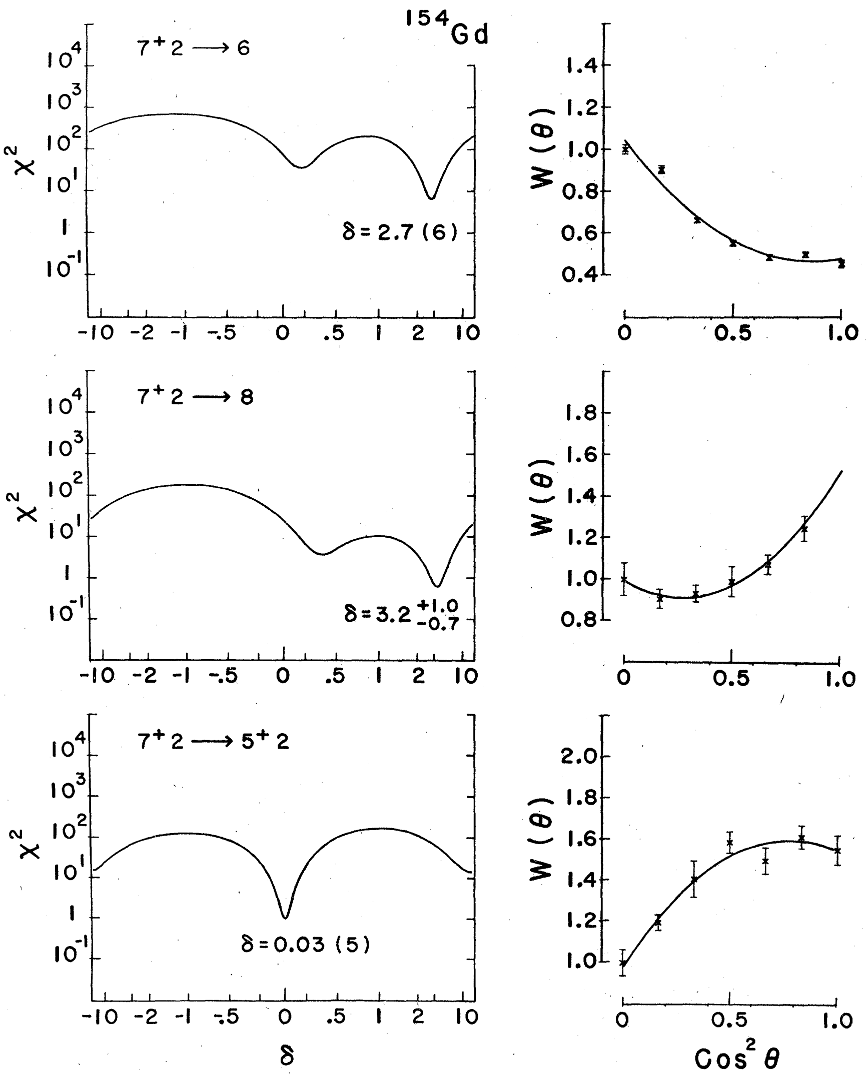

FIG. 3. Angular distribution data and typical χ^2 vs δ plots for transitions from the proposed 7^+ state in the γ band of ^{154}Gd.

tions of 897 keV ($9\rightarrow 8_g$) and 845 keV ($11\rightarrow 10_g$) and a coincident transition of 441 keV between these states. Angular distribution results for the interband transitions are consistent with pure dipole character and those for the intraband transition with pure quadrupole.

An E vs $I(I+1)$ plot of these proposed negative parity states is shown in Fig. 5(b). Considering this (and also Fig. 2) it can be seen that the spin 7, 9, and 11 states are likely members of the $K^\pi=0^-$ band based at 1241.3 keV. The behavior of the E vs $I(I+1)$ dependence is very similar to that observed for the $K^\pi=0^-$ bands in ^{162}Er (Ref. 24) and the $N=90$ nucleus ^{156}Dy (Ref. 25). If the energies of the spin 7, 9, and 11 states are fitted to Eq. (1), an A value of 11.3 keV is obtained ($B=-3.6$ eV), and the spin 5 state would subsequently be expected at 1388 keV, as compared to the experimental value of 1364 keV.

It is of interest to note that the ratio $B(E1;11^- \rightarrow 10_g^+)/B(E2;11^-\rightarrow 9^-)$ is 1.65 (13) $\times 10^{-5}$ b^{-1}. This is consistent with values measured by Zolnowski *et al.*[26] for the analogous state of $K^\pi=0^-$ bands in the transitional nuclei ^{152}Gd and ^{156}Er.

$K^\pi=7^-$ band at 2137.8 keV. The in-beam delayed coincidence data indicated that transitions of 131, 165, 172, 246, 260, 266.0 (composite), and 303 (composite) keV preceded the isomeric state at 2137.8 keV ($T_{1/2}=68$ nsec). This state has been assigned previously as $\{\frac{3}{2}^+[651\uparrow]-\frac{11}{2}^-[505\uparrow]\}_n$.[13] The

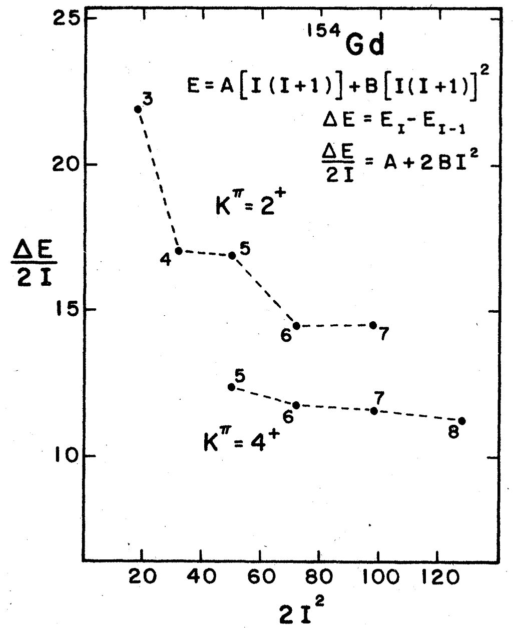

FIG. 4. Plots of $\Delta E/2I$ vs $2I^2$ for the γ-vibrational band and the $K^\pi = 4^+$ band based at 1646 keV in ^{154}Gd.

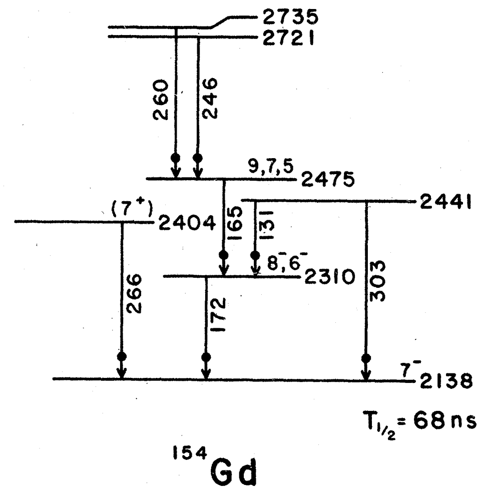

FIG. 6. Partial decay scheme involving transitions which precede the 68 ns state at 2138 keV in ^{154}Gd. All transitions have been placed on the basis of coincidence data.

partial decay scheme shown in Fig. 6 is based on our prompt and delayed coincidence spectra and also on angular distribution data for the 165 and 172 keV transitions. The states at 2310 and 2475 keV are the most likely candidates for the 8^- and 9^- levels of a band based on the 2137.8 keV 7^- state. The angular distribution data are consistent only with assignments of 6^- or 8^- for the 2310 keV state, which then lead to assignments of 5^-, 7^-, or 9^- for the 2475 keV state. The composite nature of the "303" keV transition depopulating the 2441 keV level precludes any spin-parity information for that level, which in any case is a less likely candidate (on the basis of energy arguments) for the 9^- member of the 7^- band. None of the proposed states in the $K^\pi = 7^-$ band nor the 2441 keV state have been observed in the neutron transfer experiments of Jolly and Waddington.[21]

The band parameters obtained from a fit to Eq. (1) are shown in Table IV. The A coefficient is 12.1 keV, a value which is comparable to that

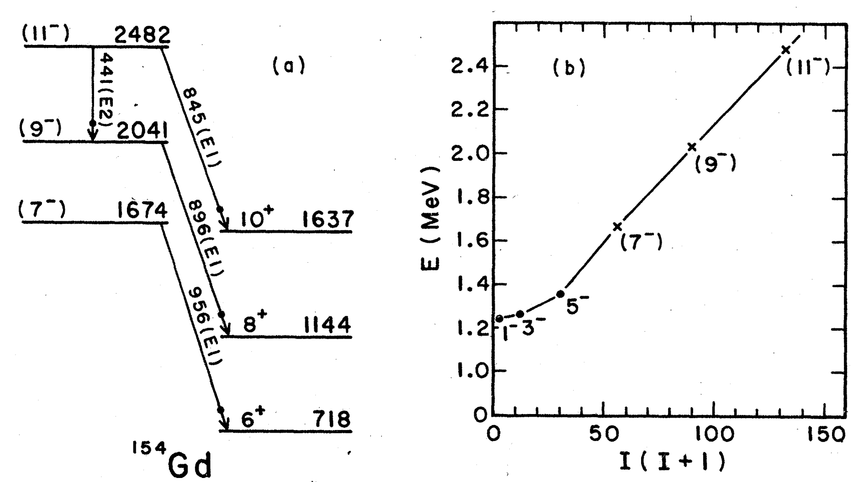

FIG. 5. (a) Partial decay scheme showing the depopulation of the proposed 7^-, 9^-, and 11^- states in the $K^\pi = 0^-$ band. (b) Plot of E vs $I(I+1)$ for states in this band.

found for the $K^\pi = 4^+$ band but significantly smaller than the value of 21.4 keV for the ground-state band. It is not practical to obtain an estimate for the inertial parameter expected for a band based on this two-neutron quasiparticle state as was done for the $K^\pi = 4^+$ band.

The only high-spin states in this region of the excitation spectrum which are observed in both the $(\alpha, 2n\gamma)$ and the neutron-transfer experiments are those at 2404 and 2735 keV. The composite character of the 266 keV transition depopulating the 2404 keV state precludes any spin-parity information from our experiments, but Jolly and Waddington have proposed a $(7^+, 7)\ \{\frac{3}{2}^-[521] + \frac{11}{2}^-[505]\}_n$ assignment. The state at 2735 keV deexciting via a 260 keV transition to the 2475 keV state (tentatively 9^-) has been assigned by Jolly and Waddington as the 8^- member of the strongly Coriolis mixed $\{\frac{5}{2}^+[413] + h_{11/2}\}_p$ configuration. They place the 7^- and 6^- states at 2570 and 2432 keV, respectively, but we observe neither of these two states.

IV. DISCUSSION

A. Positive-parity bands

One motivation for undertaking this study of ^{154}Gd was to search for the possible "superband" postulated by Khoo *et al.*[16] which would be expected to intersect the β band at about spin 12. A plot of E vs $I(I+1)$ for levels in four positive-parity bands is shown in Fig. 7, and no evidence for such an intersecting band is seen.

TABLE V. z_2 parameters describing mixing of γ-vibrational and ground-state bands in ^{154}Gd.

Level energy (keV)	$\frac{I_iK_i \to I_fK_F}{I_iK_i \to I_f'K_f}$	$z_2 \times 10^2$ Present work	$z_2 \times 10^2$ Other
996.3	$\frac{22 \to 00}{22 \to 20}$		7.3(7) [a]
	$\frac{22 \to 20}{22 \to 40}$		11.1(10) [a]
	$\frac{22 \to 00}{22 \to 40}$		9.3(5) [a]
1127.6	$\frac{32 \to 20}{32 \to 40}$	9.9(7)	7.2(4) [a]
1263.9	$\frac{42 \to 20}{42 \to 44}$		0.54(5) [a]
1432.5	$\frac{52 \to 40}{52 \to 60}$	7.8(6)	4.2(12) [b]
1606.8	$\frac{62 \to 40}{62 \to 60}$		4.5(6) [b]
1810.3	$\frac{72 \to 60}{72 \to 80}$	5.2(5)	
Weighted average for odd-spin states		6.3(3)	6.9(3)

[a]Taken from Ref. 2.
[b]Taken from Ref. 14.

Considerable odd-even staggering is observed for the γ band, as can be seen in Fig. 4. The even-spin members are depressed in energy relative to the odd-spin members similar to the case of the isotone $^{156}_{66}$Dy (Ref. 25). This might indicate that mixing of the γ band with the ground-state (g.s.) and β bands is less than mixing with other excited $K=0$ bands lying above the γ band.

An analysis of the mixing between the γ and g.s. bands was carried out in the customary manner,[27] introducing the band-mixing parameter z_2. There were sufficient γ-ray intensity data to obtain z_2 values associated with the 3^+, 5^+, and 7^+ states of the γ band and these results are listed in Table V. The weighted average of the z_2 values agrees within errors with that obtained by previous investigators even though the invividual z_2 values do not overlap within errors. It may be noted that El Masri *et al.*[25] found that the various z_2 values did not agree in the case of ^{156}Dy either. After carrying out extensive analyses, they concluded that no existing theoretical approaches could reproduce the available data on the γ-ray transition probabilities in the decay of various members of the β and γ bands in ^{156}Dy.

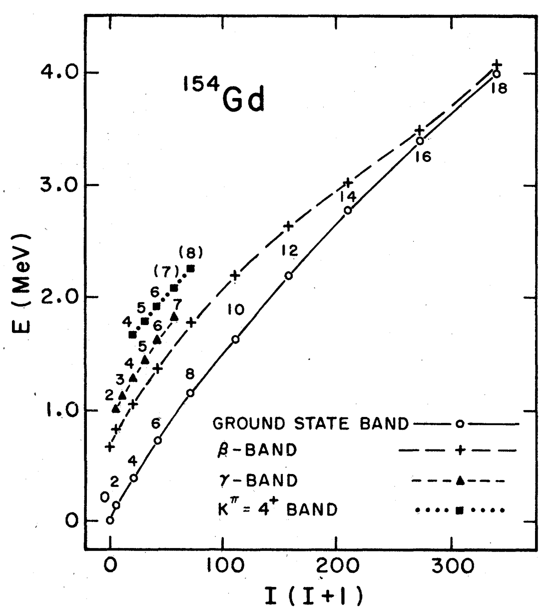

FIG. 7. Plots of E vs $I\,(I+1)$ for four positive-parity bands.

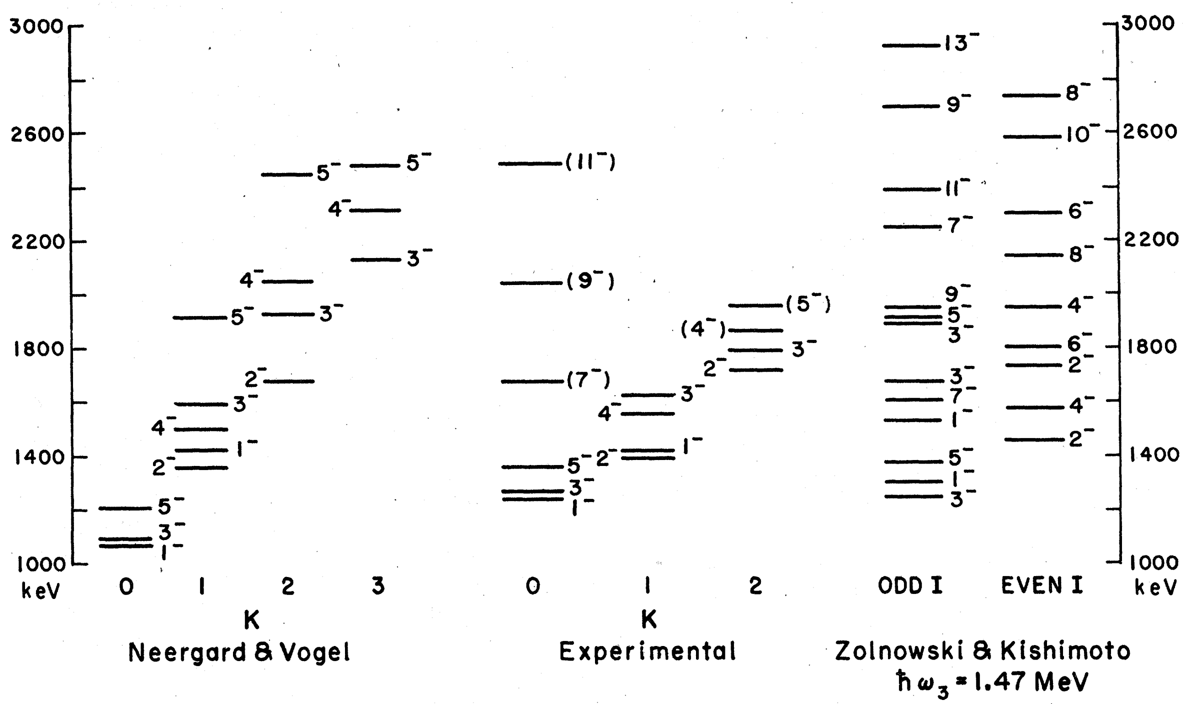

FIG. 8. Comparison of negative-parity octupole vibrational states in ^{154}Gd with the theoretical predictions of Neergard and Vogel (Ref. 28) and Zolnowski and Kishimoto (Ref. 32).

B. Negative-parity bands

Several different theoretical approaches have been made in attempts to describe negative-parity bands in this mass region. Tke model of Neergard and Vogel[28] involved random-phase approximation (RPA) calculations of low-lying octupole states incorporating an octupole-octupole force and Coriolis coupling between the lowest $K^\pi = 0^-$ to 3^- bands. Considerable success has been attained in predicting level energies and $B(E3)$ values in doubly even deformed nuclei. Vogel[29] has recently extended the calculations to the higher-spin members of these bands for several nuclei. He considers two different approaches, one of which is a model where two-quasiparticle states are coupled to a rotating core. He found that above a critical spin value the negative-parity states should be regarded as decoupled two-quasiparticle states. The application of this model to ^{162}Er has been described in detail by Janssens *et al.*[24] but unfortunately no calculations using this approach are available for ^{154}Gd.

Zolnowski, Kishimoto and co-workers[30-32] have carried out calculations for several nuclei using a model where an octupole vibration is coupled to a rotating quadrupole core [quadrupole-octupole coupling (QOC)]. The one-phonon octupole energy and the strength parameter K of the quadrupole-octupole coupling are the only free parameters. The interacting boson approximation (IBA) model of Iachello and Arima[33] is a similar approach to the problem and essentially differs from that of Zolnowski *et al.* in the choice of H_{coupl} and the fact that it requires five parameters to describe the splitting of the quadrupole-octupole multiplet states.

A comparison between the available data for ^{154}Gd and the theoretical predictions of Neergard and Vogel[28] and Zolnowski *et al.*[32] is shown in Fig. 8. The $\hbar\omega_3$ value was 1.47 MeV for the QOC calculations; it can be seen that the predictions for the first 7^-, 9^-, and 11^- states from this calculation are in reasonable agreement with our experimental results.

The authors wish to thank Dr. A. Visvanathan and Dr. E. Marshalek for helpful discussions and Dr. John Fleissner and David Rakel for their assistance. We especially wish to thank Dr. D. Zolnowski for providing the most recent results of his calculations. This work was supported in part by the National Science Foundation, Grant No. PHY 76-23352.

*Present address: Applied Physics Laboratory, Johns Hopkins University, Silver Spring, Maryland.

[1]L. Varnell, J. D. Bowman, and J. Trischuk, Nucl. Phys. A127, 270 (1969).
[2]G. E. Keller and E. F. Zganjar, Nucl. Phys. A153, 647 (1970).
[3]L. L. Riedinger, N. R. Johnson, and J. H. Hamilton Phys. Rev. C 2, 2358 (1970).
[4]R. A. Meyer, Phys. Rev. 170, 1089 (1968); 174, 1478 (1968).
[5]P. Gottel, W. Delang, and H. Seyfarth, Z. Phys. 255, 450 (1972).
[6]J. H. Hamilton, A. V. Ramayya, and L. C. Whitlock, Phys. Rev. Lett. 22, 65 (1969); 23, 1178 (1969).
[7]N. Rud and K. Bonde Nielsen, Nucl. Phys. A158, 546 (1970).
[8]L. C. Whitlock, J. H. Hamilton, and A. V. Ramayya, Phys. Rev. C 3, 313 (1971).
[9]J. Lange, R. L. Rasera, H. F. Wagner, and W. Schaffner, Nucl. Phys. A171, 92 (1971).
[10]L. Marinkov, I. Bikit, I. Anicin, M. Zupancic, D. Cveticannin, R. Stepic, and R. Vukanovic, Z. Phys. 248, 345 (1971).
[11]D. R. Ober, W. Weeber, and R. L. Place, Phys. Rev. C 7, 738 (1973).
[12]J. B. Gupta, S. L. Gupta, J. H. Hamilton, and A. V. Ramayya, Z. Phys. A282, 179 (1977).
[13]L. L. Riedinger, D. C. Sousa, E. G. Funk, and J. W. Mihelich, Phys. Rev. C 4, 1352 (1971).
[14]D. C. Sousa, L. L. Riedinger, E. G. Funk, and J. W. Mihelich, Nucl. Phys. A238, 365 (1975).
[15]T. S. Vylov, I. I. Gromova, V. V. Kuznetzov, V. G. Nedovesov, V. I. Forminykh, Uy. V. Kholnov, and G. E. Schhukin, Izv. Akad. Nauk SSSR, Ser. Fiz. 36, 718 (1972) [Bull. Acad. Sci. USSR Phys. Ser. 36, 649 (1972)].
[16]T. L. Khoo, F. M. Bernthal, J. S. Boyno, and R. A. Warner, Phys. Rev. Lett. 31, 1146 (1973).
[17]S. M. Ferguson, R. Heffner, and H. Ejiri, Phys. Lett. 35B, 214 (1971).
[18]I. Rezanka, F. M. Bernthal, J. O. Rassmussen, R. Stokstad, I. Fraser, J. Greenberg, and D. A. Bromley, Nucl. Phys. A179, 51 (1972).
[19]D. Ward, R. L. Graham, J. S. Geiger, and H. R. Andres, Phys. Lett. 44B, 39 (1973).
[20]R. Bloch, B. Elbek, and P. O. Tjom, Nucl. Phys. 91, 576 (1967).
[21]O. Jolly and J. C. Waddington, (private communication).
[22]D. Cline and P. M. S. Lesser, Nucl. Instrum. Methods 82, 291 (1970).
[23]G. D. Dracoulis, J. R. Leigh, M. G. Slocombe, and J. O. Newton, J. Phys. G 1, 853 (1975).
[24]R. Janssens, Y. El Masri, J. M. Ferte, C. Michel, J. Steyaert, and J. Vervier, Nucl. Phys. A283, 493 (1977).
[25]Y. El Masri, J. M. Ferte, R. Janssens, C. Michel, P. Monseu, J. Steyaert, and J. Vervier, Nucl. Phys. A271, 133 (1976).
[26]D. R. Zolnowski, Y. Gono, and T. T. Sugihara, Cyclotron Institute, Texas A & M University, Progress Report, 1974 (unpublished), Vol. 20.
[27]L. Riedinger, N. R. Johnson, and J. H. Hamilton, Phys. Rev. 179, 1214 (1962).
[28]K. Neergard and P. Vogel, Nucl. Phys. A145, 33 (1970).
[29]P. Vogel, Phys. Lett. 60B, 431 (1976).
[30]D. R. Zolnowski, T. Kishimoto, Y. Gono, and T. T. Sugihara, Phys. Lett. 55B, 453 (1975).
[31]D. R. Zolnowski, H. Beuscher, and T. T. Sugihara, Z. Phys. A277, 113 (1976).
[32]D. R. Zolnowski and T. Kishimoto, Cyclotron Institute, Texas A & M University, Progress Report, 1974 (unpublished); and private communication.
[33]A. Arima and F. Iachello, Ann. Phys. N.Y., 99, 253 (1976).